Petrology, Vol. 5, No. 6, 1997, pp. 534–549. Translated from Petrologiya, Vol. 5, No. 6, 1997, pp. 596–613.

64

Metamorphic Evolution and the Composition of the Protolith of Plagioclase-bearing Eclogite-Amphibolites of the Buchim Block of the Serbo–Macedonian Massif, Macedonia

S. P. Korikovsky*, V. Mirčovski, and G. S. Zakariadze*****

* *Institute of the Geology of Ore Deposits, Petrography, Mineralogy, and Geochemistry, Russian Academy of Sciences, Staromonetnyi per. 35, Moscow, 109017 Russia; e-mail: korik@igem.msk.su*

** *Faculty of Mining and Geology, Goce Delcev 89, 92000 Stip, Macedonia*

*** *Vernadsky Institute of Geochemistry and Analytical Chemistry, Russian Academy of Sciences, ul. Kosygina 19, Moscow, 117975 Russia*

Received May 20, 1997

Abstract—Mineral equilibria are studied in plagioclase-bearing eclogite-amphibolites and associated garnet–clinopyroxene–amphibole–plagioclase crystalline schists of the Buchim Block of the Serbo–Macedonian Massif. The rocks contain the following stable minerals: clinopyroxene of the *Aug*–Na-*Aug*–*Omp* series with a *Jd* content from 5 to 34%, garnet with a distinct prograde zoning, hastingsite–tschermakite–pargasite hornblende, and oligoclase. It is shown that Na content in the coexisting *Cpx* and *Pl*, the presence of *Pl*, *Hbl*, *Cpx*, and *Grt* in the metabasites, and transition of the eclogites to eclogite-amphibolites, amphibolites, and crystalline schists are controlled only by the Na/Al, Ca : Al : (Mg, Fe), and (Na + Al)/(Mg + Fe) ratios in the rocks, and not by later feldspathization or amphibolization. The conditions of the prograde stage were as follows: $T = 650°C$, $P = 12–12.5$ kbar, depth 46–48 km, and the geothermal gradient was 14°C/km. Reaction textures, such as Cpx^2 (0–6% *Jd*) + Pl^2 (25–32% *An*) kelyphites around the omphacite and $Hbl^2 + Pl^2$ (46–73% *An*) rims around the garnet at its contact with Cpx^1 and Hbl^1 crystallized only during the late exhumation stage because of the rapid uplift under isothermal conditions or even at an inertial increase in the temperature. The effect of the (Na + Al)/(Mg + Fe) ratio in the eclogites on plagioclase presence or absence in paragenesis with *Cpx* + *Grt*, general phase equilibria in the moderate depth eclogite complexes of the plagioclase depth facies, and the boundary reaction of transition to the deeper kyanite facies of depth are considered using the example of the Buchim Block. The protolith of the eclogite–amphibolites under study is close to basalts of mid-oceanic ridges (N- and T-MORB) in composition. The magmas of this composition intruded into the thinned continental crust or sedimentary sequences covering the areas of the young oceanic crust.

GEOLOGIC SETTING

The Buchim Block, which is composed of medium- to high-temperature metamorphic rocks of various composition, is a part of the Serbo–Macedonian Massif near its contact with the Vardar zone in eastern Macedonia. The protolith of the metamorphic rocks of the Serbo–Macedonian Massif is believed to have a Late Proterozoic–Early Paleozoic age (Karamata and Krstič, 1996).

The age of metamorphism and the number of metamorphic cycles are debatable because isochron isotopic dating of these rocks was absent until recently. A Sm–Nd mineral isochron indicating a Late Hercynian age of metamorphism (260 ± 49 Ma) is obtained now by S.F. Karpenko, Vernadsky Institute of Geochemistry (personal communication) for the eclogite-amphibolites described in this paper.

The amphibole eclogites were discovered by V. Ivanova (unpublished data) and studied by Mirčovski (1991). They compose layers or boudin lenses 0.5–10 m thick in a metamorphic sequence that consists of biotite–amphibole, biotite–muscovite, and kyanite–staurolite–garnet gneisses with interlayers of garnet and clinopyroxene amphibolites and garnet–clinopyroxene–amphibole–plagioclase crystalline schists.

The amphibole eclogites and eclogite-amphibolites are concordant to and sometimes intercalate with the host gneisses and amphibolites in outcrops. However, the detailed mapping and tracing of eclogite bodies for 0.5–1 km (Mirčovski, 1991) reveal their slightly discordant setting relative to the gneiss. Apparently, this indicates the primary igneous origin of the eclogite-amphibolites, which formed during metamorphism of subsequent diabase dikes no more than a few meters thick and several hundred meters long.

These data rule out any possibility that the eclogites were implanted tectonically into the host gneisses and certainly indicate that the rocks were metamorphosed *in situ* simultaneously with surrounding rocks.

The Buchim Block is dominated by silicic, potassium-rich, mica and amphibole–biotite gneisses, which probably have a terrigenous sedimentary parentage. Only some bodies of K-feldspar-bearing orthogneisses have relics of a primary granite-porphyry texture.

PETROGRAPHY AND MINERALOGY OF ECLOGITIC ROCKS AND ASSOCIATED CLINOPYROXENE-BEARING METABASITES

The eclogitic rocks have a fine-grained granoblastic texture of the groundmass with large garnet porphyroblasts. Garnet, omphacite–augitic clinopyroxene, brownish green hornblende (5–25%), quartz, and rutile are the major primary minerals. The rocks also bear variable amounts of plagioclase (3–15%), apatite, zoisite, and titanomagnetite. All these minerals are in equilibrium.

According to the classification of eclogitic rocks (Carswell, 1990), crustal eclogite proper is a plagioclase-free rock, more than 70% of which is composed of garnet and omphacitic (chloromelanitic, jadeitic) clinopyroxene. The eclogitic rocks of the Buchim Block contain plagioclase, notable amounts of hornblende, and Na-augite, along with omphacite (Fig. 1). Hence, this rock group as a whole should be termed eclogite-amphibolites, even though some rocks of this group correspond to eclogites in composition.

Other types of garnet- and clinopyroxene-bearing metabasites are associated with eclogite-amphibolites, grade to them across the strike of eclogite bodies, or compose individual layers and bodies among the host rocks. These metabasites comprise garnet–clinopyroxene–amphibole–plagioclase crystalline schists and even gneisses, which contain up to 35% intermediate or basic plagioclase, and garnet or clinopyroxene amphibolites, some of which preserve relict gabbroic textures. Some clinopyroxene–garnet–amphibole–plagioclase crystalline schists contain scapolite and graphite, calcite inclusions in garnet, and therefore, could be formed after calc-silicate metasedimentary rocks.

All these metabasites pervasively have the following five equilibrium rock-forming minerals: clinopyroxene, garnet, hornblende, plagioclase, and quartz. Therefore, the eclogite-amphibolites are not the alien nonequilibrium rocks among the metamorphites of the Buchim Block. These rocks form a group of cognate metabasites of the Buchim Block, which differ from one another only by mineral proportions and compositions. So, the rock mineralogy and phase equilibria of the prograde stage are discussed below together with eclogite-amphibolites and other metabasites.

Minerals of the Prograde Stage

Microprobe analyses of minerals were obtained with a CamScan electron microscope at the Geological Faculty of the Moscow State University.

Clinopyroxene. Clinopyroxene is one of the major minerals of eclogite-amphibolites and crystalline schists and occurs as equant grains. Its composition in the eclogite-amphibolites varies significantly within the ranges 5–34% *Jd* and 5–15% *Ac* (Table 1). It is fairly magnesian and has low X_{Fe} values of 0.13–0.19. Clinopyroxene from the garnet–clinopyroxene–

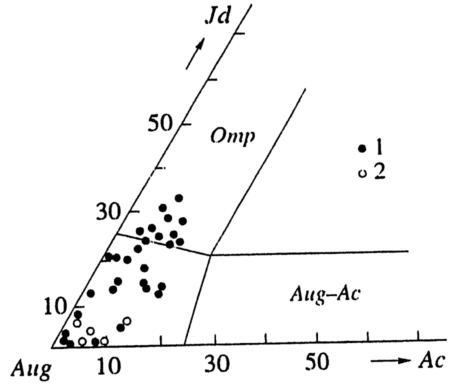

Fig. 1. Composition of primary clinopyroxene (1) from the groundmass of eclogite-amphibolites and *Grt–Cpx–Hbl–Pl* crystalline schists and secondary clinopyroxene (2) from Cpx^2–Pl^2 kelyphites around omphacite.

amphibole–plagioclase crystalline schists has very low *Jd* (0–3%) and *Ac* (0–8%) contents, and significantly higher X_{Fe} = 0.25–0.51. Figure 1 shows that the primary clinopyroxenes from the metabasites compose a continuous series *Aug*–Na-*Aug*–low-Na *Omp*. Their composition, Fe mole fraction among other parameters, is controlled by the rock composition (see below). Clinopyroxene grains are homogeneous, usually without zoning.

Garnet. All garnets of eclogite-amphibolites, even those rimmed by secondary hornblende, have a typical prograde zoning along the whole profile across the grains with a Mg increase and Ca decrease from the core to margin (Table 2). For example, in Sample 9E, the pyrope content increases toward the margins from 13 to 35%, and grossular decreases from 27 to 16% (Fig. 2). All the garnets can be classified with the pyrope–almandine–grossular series low in Mn. The X_{Fe} value decreases in grain margins to 0.55.

Most garnets in the garnet–clinopyroxene–amphibole–plagioclase crystalline schists and amphibolites also have a prograde zoning. For instance, the pyrope content in the garnet of Sample 6/2 (Table 2) increases toward the margin from 13 to 20%, and the content of grossular slightly decreases. However, a specific retrograde zoning was revealed in some garnet grains of these rocks, where grossular increases and pyrope slightly decreases toward the margins (Sample 21, Table 2, Fig. 2).

The garnets in crystalline schists are generally higher in X_{Fe} (up to 0.89) and show somewhat higher Ca mole fraction than this mineral in the eclogite-amphibolites (X_{Fe} = 0.55–0.63 in grain margins), i.e., their composition, like that of *Cpx*, is definitely controlled by the bulk composition of the rocks.

Hornblende. Prismatic grains of the primary hornblende are brownish green. They are variable in composition, particularly in X_{Fe}, Na_B, and $(Na + K)_A$ values (Table 3). All of them are classified with Al-rich calcic amphiboles: hastingsite, pargasite, and tschermakite hornblende (Rock and Leake, 1984). The primary Ca-amphiboles in various metabasites differ in Fe mole

Table 1. Representative microprobe analyses of primary clinopyroxene (Cpx^1) from eclogite-amphibolites and clinopyroxene–garnet–amphibole–plagioclase crystalline schists

Component	9E			6		26E		21		12	6/2	9/2	
SiO_2	51.55	52.05	52.52	51.05	50.20	52.14	52.25	50.12	49.38	52.23	52.58	53.48	52.82
TiO_2	0.53	0.52	0.49	0.41	0.49	0.31	0.43	0.19	0.44	0.56	0.22	0.32	0.28
Al_2O_3	7.07	8.94	8.12	6.06	6.13	9.89	10.52	2.34	4.83	10.64	3.44	11.61	11.37
Fe_2O_3	3.99	5.48	4.74	0.36	2.86	3.66	4.41	1.03	1.04	2.94	–	2.96	4.06
FeO	4.85	3.22	3.75	7.40	6.34	3.48	2.71	15.40	13.63	2.67	8.20	2.77	2.50
MnO	0.08	–	0.02	0.13	0.34	0.12	0.09	0.02	0.01	–	0.14	0.04	–
MgO	12.13	9.89	10.54	12.81	12.19	9.76	8.61	8.30	8.17	9.71	12.53	8.26	8.64
CaO	17.28	15.88	15.87	20.91	20.21	16.50	15.74	22.22	21.78	16.75	22.72	14.21	14.34
Na_2O	2.85	4.54	4.26	0.84	1.12	4.48	5.25	0.47	0.82	4.47	0.55	6.11	5.86
K_2O	–	0.03	0.05	0.01	0.10	–	–	–	–	–	0.01	–	–
Total	100.32	100.55	100.36	99.98	99.98	100.35	100.0	100.09	99.77	99.97	100.39	99.75	99.87
Si	1.87	1.88	1.90	1.88	1.87	1.88	1.89	1.92	1.87	1.89	1.94	1.92	1.90
Ti	0.01	0.01	0.01	0.01	0.01	0.01	0.01	0.01	0.01	0.02	0.01	0.01	0.01
Al	0.31	0.38	0.35	0.27	0.27	0.42	0.45	0.11	0.22	0.45	0.15	0.49	0.48
Fe^{3+}	0.11	0.15	0.13	0.01	0.08	0.10	0.12	0.03	0.03	0.08	–	0.08	0.11
Fe^{2+}	0.15	0.10	0.11	0.23	0.20	0.11	0.08	0.50	0.44	0.08	0.26	0.08	0.08
Mn	–	–	–	–	0.01	–	–	–	–	–	–	–	–
Mg	0.66	0.54	0.57	0.71	0.67	0.53	0.46	0.48	0.47	0.52	0.70	0.44	0.46
Ca	0.68	0.62	0.62	0.83	0.80	0.64	0.61	0.92	0.90	0.65	0.91	0.55	0.55
Na	0.20	0.32	0.30	0.06	0.08	0.31	0.37	0.04	0.06	0.31	0.04	0.43	0.41
K	–	–	–	–	–	–	–	–	–	–	–	–	–
Jd	5.0	14.0	15.0	2.0	–	17.0	23.6	–	–	23.2	3.0	33.8	28.6
Ac	11.0	15.0	13.0	1.0	8.2	10.0	12.2	3.0	3.0	8.1	–	8.1	11.1
Aug	84.0	71.0	72.0	97.0	91.8	73.0	64.2	97.0	97.0	68.7	97.0	58.1	60.3
$X_{Fe^{2+}}$	0.19	15.0	0.17	0.25	0.23	0.17	0.15	0.51	0.48	0.13	0.27	0.16	0.14

Note: The numbers of cations are calculated on the basis of 6 oxygens and 4 cations. In Tables 1, 5, and 7: Fe_2O_3 and Fe^{3+} are calculated by charge balance. In all tables: eclogite-amphibolites are Samples 9E, 9/2, 9/3, 12, 26E, *Cpx–Grt–Hbl–Pl* crystalline schists are Samples 6, 6/2, 21. In Tables 1–7 and 9: oxides are in wt %.

fraction. Hornblende has $X_{Fe} = 0.32–0.43$ in the eclogite-amphibolites, and $X_{Fe} = 0.39–0.78$ in the crystalline schists. The brownish green color of all primary hornblendes is caused by their high Ti contents (Fig. 3).

Plagioclase. The primary plagioclases form individual equant grains in the groundmass of the eclogite-amphibolites being in equilibrium with omphacite and Na-augite. All of the plagioclases are oligoclase and contain 12–27% *An* (Table 4). The plagioclase in the crystalline schists is more calcic (andesine–labradorite with 28–51% *An*).

Mineral Assemblages of the Prograde Stage

Correlation between the compositions of coexisting clinopyroxene and primary plagioclase in the eclogite-amphibolites and crystalline schists point to very important relationships. The most sodic omphacites associate with more sodic plagioclases, whereas the less sodic clinopyroxenes (augites) coexist with andesine-labradorite (Fig. 4). $Cpx^1–Pl^1$ tie lines do not intersect and are nearly parallel in a Na–Ca–(Mg, Fe) diagram, indicating that (a) the Ca and Na distribution between the two phases corresponds to approximately the same temperature and depends only on the Na/Ca ratio in the rocks, and (b) the eclogitic rocks are affiliated with the same facies as the *Grt–Cpx–Hbl–Pl* crystalline schists and gneisses do. Obviously, the Na/Ca ratio in the andesine- and labradorite-bearing crystalline schists is relatively low and causes the low-Na clinopyroxene (augite) composition in them. The eclogite-amphibolites containing oligoclase or albite–oligoclase have a higher Na/Ca ratio and, hence, bear the Na-richest clinopyroxenes.

The prograde phase equilibria in the eclogite-amphibolites and their mineral compositions are shown in an ACF diagram (Fig. 5) as a projection from the point of oligoclase. Taking into account that similar amphiboles, clinopyroxenes, garnets, and plagioclases also occur in the other metabasites, and using this diagram, we can explain why the eclogitic rocks, garnet and clinopyroxene amphibolites, and plagioclase-rich crystalline schists that seem to contain alternative mineral assemblages are in equilibrium within the same metamorphic complex of the Buchim Block. According to Fig. 5, the metabasites slightly enriched in Ca and Al should contain the $Cpx^1 + Grt$ assemblage (field 1), which corresponds to amphibole-free clinopyroxene–garnet eclogites or crystalline schists with variable, if any, *Pl* content. The rocks somewhat richer in Mg and Fe should contain the $Cpx^1 + Hbl^1$ assemblage (field 2) typical of garnet-free clinopyroxene amphibolites and crystalline schists. The $Grt + Hbl^1$ (field 3) clinopyroxene-free assemblage is typical of the rocks lowest in Ca such as ordinary garnet amphibolites. At an intermediate Ca : Al : (Mg, Fe) ratio, the rocks contain three-mineral $Cpx^1 + Grt + Hbl^1$ assemblage with plagioclase and quartz. This assemblage is typical of the hornblende eclogites and eclogite-amphibolites of the Buchim Block.

Thus, the variations in the mineralogy of the rocks and the compositions of minerals in the metabasites of the Buchim Block, which were only slightly affected by retrograde processes, can be easily explained by the primary, rather small, differences in major-element contents of their protolith, for example by variation in Na/Ca, Ca : Al : (Mg, Fe), and (Na + Al)/(Mg + Fe). Therefore, the variability of the metabasites does not reflect different *P–T* conditions of their crystallization.

The eclogite-amphibolites compose one geologic complex with surrounding rocks and bear evidence of only one prograde metamorphic stage. We can conclude, therefore, that eclogites, amphibolites, crystalline schists, and gneisses of the Buchim Block are metamorphosed within one cycle and under similar *P–T* conditions.

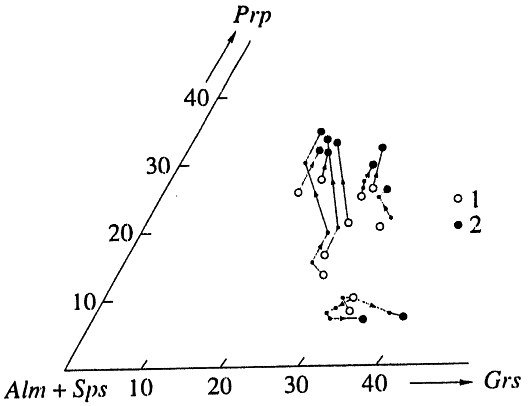

Fig. 2. Variation of garnet composition from grain cores (1) to rims (2).

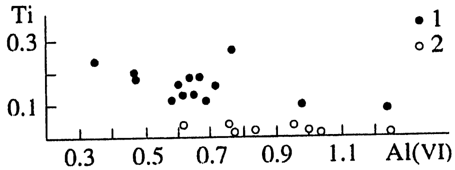

Fig. 3. Covariance of Ti and Al(VI) in primary (1) and secondary (2) pargasite–hastingsite–tschermakite hornblendes from eclogite-amphibolites.

Reactional Textures Related to the Uplift and the Onset of the Retrograde Stage

The eclogitic rocks of the Buchim Block usually bear reaction textures that indicate an evolution of the conditions after the peak of prograde metamorphism.

The retrograde alterations will be considered below only for eclogite-amphibolites, because the *P–T* trends of subsequent metamorphic stages are most pronounced in composition of these rocks.

The first type of textures comprises fine-grained or even cryptocrystalline clinopyroxene–plagioclase kelyphitic rims around omphacite. Their crystallinity is so fine that they are black and look like isotropic under the microscope, and their minerals can hardly be identified.

Table 2. Representative microprobe analyses of zoned garnet

Component	9E			9/2		12			26E		6/2		21	
	c	*m*	*r*	*c*	*r*	*c*	*m*	*r*	*c*	*r*	*c*	*r*	*c*	*r*
SiO_2	38.26	39.30	39.28	38.25	38.45	39.14	39.60	39.34	38.92	39.31	38.41	38.65	37.87	37.29
TiO_2	0.18	–	0.04	–	–	0.11	0.11	0.06	0.01	0.01	0.27	0.14	0.18	0.17
Al_2O_3	22.43	22.81	23.19	21.85	22.08	21.60	21.56	21.57	22.63	22.84	20.78	21.23	21.40	20.93
FeO	25.45	23.78	22.14	23.11	23.14	21.49	20.82	19.16	21.42	20.07	21.73	21.57	26.22	24.05
MnO	1.11	0.62	0.32	1.62	0.37	0.78	0.53	0.31	0.94	0.59	2.40	0.90	0.58	0.25
MgO	3.28	7.62	8.92	5.46	8.91	6.82	7.60	8.77	5.16	6.67	3.22	5.07	2.28	1.67
CaO	9.28	5.81	5.88	9.55	6.67	10.01	9.94	9.73	10.72	10.34	12.68	11.97	11.46	14.22
Total	99.99	99.40	99.72	99.84	99.60	99.95	100.16	98.94	99.80	99.83	99.49	99.53	99.99	98.58
Alm	57.4	52.3	48.5	49.5	48.2	46.0	44.0	40.0	47.3	43.8	47.0	46.0	57.6	52.9
Sps	2.5	1.4	0.7	3.5	0.8	2.0	1.0	1.0	2.1	1.3	5.0	2.0	1.3	0.5
Prp	13.2	29.9	34.8	20.8	33.1	26.0	29.0	33.0	20.3	26.0	13.0	20.0	8.9	6.6
Grs	26.8	16.4	16.0	26.2	17.9	27.0	26.0	25.0	30.3	28.9	35.0	32.0	32.2	40.0
X_{Fe}	0.81	0.64	0.58	0.70	0.59	0.64	0.61	0.55	0.73	0.63	0.79	0.70	0.87	0.89

Note: core (*c*), transitional zones (*m*), rim (*r*).

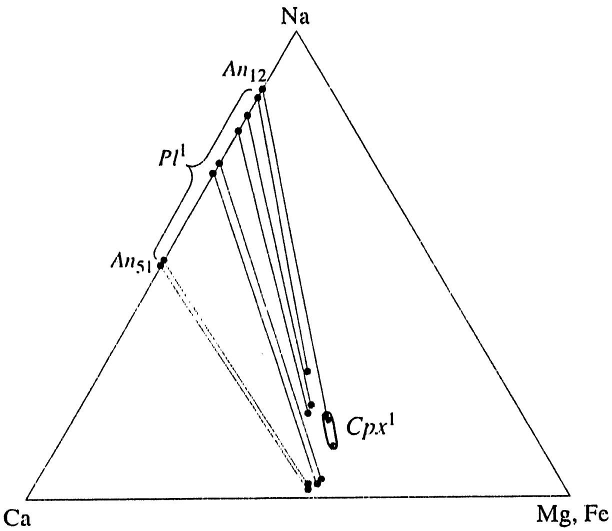

Fig. 4. Compositions of coexisting primary clinopyroxenes and plagioclase in eclogite-amphibolites and *Grt–Cpx–Hbl–Pl* crystalline schists plotted in a diagram Na–Ca–(Mg, Fe).

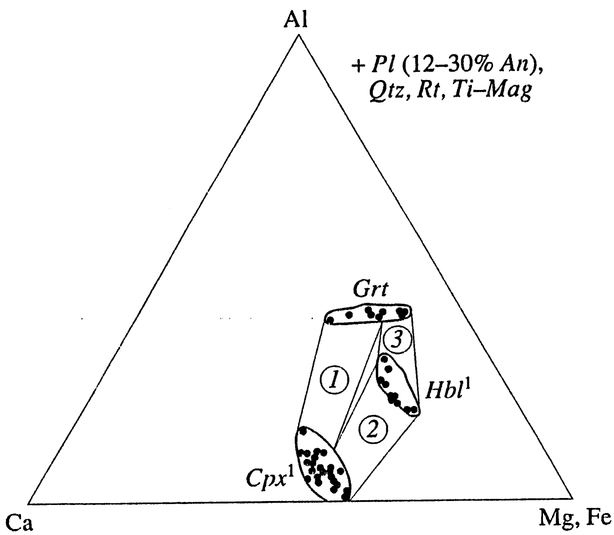

Fig. 5. Phase equilibria of garnet, primary clinopyroxene, and hornblende in eclogite-amphibolites (projection from the point of primary oligoclase).

(*1–3*) Mineral assemblages in rocks with different Ca : Al : (Mg, Fe) ratios (see text).

An electron microscope study of these rims reveals symplectitic intergrowths of Cpx^2 and Pl^2. The secondary clinopyroxene has distinctly lower *Jd* content (0.1–6%) than the primary omphacite. Analyses of some omphacite grains and minerals from kelyphitic rims around them are listed in Table 5. The plagioclase in the symplectite is oligoclase–andesine and has a higher *An* content compared to the primary plagioclase in the groundmass. The compositional relationships between the primary omphacite and the secondary $Cpx^2 + Pl^2$ assemblage (Fig. 6) show that the omphacite breakdown is caused by the isochemical reaction $Cpx^1 \longrightarrow Cpx^2 + Pl^2$.

Another type of the reaction textures in the eclogite-amphibolites and crystalline schists comprises kelyphitic rims around garnet grains at their contacts with primary clinopyroxene and hornblende. These rims consist of bluish green hornblende with symplectitic ingrowths of plagioclase. These Ca-amphiboles differ from the primary amphibole by their lower Ti (Fig. 3), higher Al, and lower Si contents (Table 6). The amphibole type, however, does not change: they are classified with ordinary or subsilicic pargasites and hastingsite (Rock and Leake, 1984). Therefore, the lower Ti content of the secondary amphibole is related to the low Ti in the interacting garnet and omphacite rather than to a temperature decrease. The plagioclase in these kelyphites is labradorite-bytownite with 46–73% *An*. The amphibole and plagioclase compositions in kelyphites from eclogite-amphibolites (Samples 26E, 9/3, 21, and 12) and crystalline schists (Samples 6, 6/2, and 21) are fairly similar (Table 6). Relationships between the primary and secondary minerals in an ACF diagram (Fig. 7) show that the Hbl^2–Pl^2 rims are not generated at the expense of garnet alone but are produced by a reaction between the garnet and neighboring omphacite and primary Ca-amphibole:

$$Grt + Cpx^1 + Hbl^1 \longrightarrow Hbl^2 + Pl^2(An_{46-73}).$$

In addition to these bimineral reactional textures, all the metabasites often show marginal replacement of primary brownish green amphiboles by secondary bluish green varieties.

P–T CONDITIONS OF THE PROGRADE STAGE AND INTERPRETATION OF THE REACTIONAL STRUCTURES

We used garnet–clinopyroxene thermometry to estimate the conditions of the prograde metamorphic stage of eclogite-amphibolite crystallization; the garnet–hornblende thermometer is less useful, because the primary amphiboles are often altered near their contacts with garnet during the retrograde stage, and, as a result, the temperature estimates involve large errors.

We employed the compositions of the outer prograde zones of garnet grains and contacting primary clinopyroxene from the groundmass for *Grt–Cpx* thermometry. Additionally, we used *Cpx* inclusions in progressively zoned garnet grains (Table 7), which correspond to the conditions near but not exactly at the peak of metamorphism. The results of calculations are listed in Table 8. The thermometers of Schliestedt (1986), Ellis and Green (1979), and Krogh (1978) are the most reliable for the use in crustal eclogites, whereas thermometers of Sengupta *et al.* (1989) and Pattison and Newton (1989) are the best for crystalline schists with low-Na clinopyroxenes. Despite the varia-

Table 3. Representative microprobe analyses of primary brownish green hornblende (*Hbl*[1])

Component	9E		6	26E	21				12		6/2		9/3	
SiO_2	43.99	43.19	43.43	39.15	40.76	39.70	39.33	41.87	38.71	42.02	43.91	42.97	41.42	42.23
TiO_2	1.68	1.84	2.06	2.23	0.96	1.10	0.98	0.83	0.95	1.65	1.18	1.48	1.45	1.74
Al_2O_3	13.41	13.63	11.80	17.52	13.99	13.83	13.81	16.91	19.41	14.89	12.40	13.55	14.86	14.98
FeO	11.95	12.58	15.13	13.78	24.35	25.48	25.97	19.33	13.76	10.97	14.91	13.04	13.84	12.31
MnO	–	–	0.24	0.14	0.06	0.13	0.05	0.15	0.19	0.06	0.23	0.10	0.19	0.05
MgO	13.90	13.28	11.77	10.42	4.89	4.27	4.14	5.59	10.20	13.25	10.70	11.29	11.64	12.36
CaO	9.02	9.59	10.92	11.37	11.13	11.28	0.77	10.81	10.70	11.37	12.06	11.79	10.58	10.57
Na_2O	3.08	3.33	1.47	3.08	1.52	1.25	1.66	1.40	3.26	3.22	1.54	1.41	3.19	3.34
K_2O	0.73	0.71	1.15	0.46	1.33	1.42	1.35	1.50	0.55	0.81	1.22	1.71	0.60	0.60
Total	97.76	98.15	97.97	98.15	98.99	98.46	98.06	98.39	97.84	98.24	98.15	97.34	97.77	98.18
Si	6.23	6.18	6.33	2.74	6.19	6.10	6.07	6.26	5.65	6.09	6.49	6.36	6.05	6.11
Al(IV)	1.77	1.82	1.67	2.26	1.81	1.90	1.93	1.74	2.35	1.91	1.51	1.64	1.95	1.89
Al(VI)	0.47	0.47	0.35	0.77	0.69	0.61	0.58	1.23	0.98	0.63	0.65	0.72	0.60	0.66
Ti	0.18	0.20	0.23	0.25	0.11	0.13	0.11	0.09	0.10	0.18	0.13	0.16	0.16	0.19
Fe^{3+}	1.22	0.97	0.84	0.46	0.58	0.67	0.80	0.17	0.80	0.35	0.12	0.12	0.72	0.54
Fe^{2+}	0.19	0.53	1.00	1.23	2.51	2.60	2.55	2.24	0.88	0.98	1.72	1.49	0.97	0.95
Mn	–	–	0.03	0.02	0.01	0.02	0.01	0.02	0.02	0.01	0.03	0.01	0.02	0.01
Mg	2.93	2.83	2.55	2.28	1.11	0.98	0.95	1.24	2.22	2.86	2.35	2.49	2.53	2.66
Ca	1.37	1.47	1.70	1.79	1.81	1.86	1.78	1.73	1.67	1.76	1.91	1.87	1.65	1.64
Na	0.85	0.92	0.41	0.88	0.45	0.37	0.50	0.41	0.92	0.90	0.44	0.40	0.90	0.94
K	0.13	0.13	0.21	0.09	0.26	0.28	0.27	0.29	0.10	0.15	0.23	0.32	0.11	0.11
$X_{Fe\,tot}$	0.33	0.35	0.42	0.43	0.74	0.77	0.78	0.66	0.43	0.32	0.44	0.39	0.40	0.36
Na_B	0.63	0.53	0.27	0.20	0.18	0.13	0.21	0.25	0.31	0.22	0.06	0.12	0.32	0.36
$(Na+K)_A$	0.35	0.52	0.36	0.77	0.52	0.52	0.55	0.44	0.72	0.82	0.61	0.61	0.69	0.69

Note: The numbers of cations are calculated on the bases of 23 oxygens and 13 cations (without Ca, Na, and K).

Table 4. Microprobe analyses of primary plagioclases (*Pl*[1])

Component	9E		6		26E	21		12	6/2	9/3	9/2
SiO_2	64.79	64.66	60.02	60.48	60.98	54.88	55.69	63.98	61.57	62.58	64.37
Al_2O_3	21.68	33.37	25.54	24.46	24.66	28.58	28.82	22.11	24.63	23.47	22.10
CaO	2.55	2.47	6.06	6.12	5.79	10.23	9.62	3.80	6.27	4.50	3.07
Na_2O	10.15	9.77	7.74	8.41	8.51	5.51	5.53	9.27	7.82	9.29	10.19
K_2O	0.30	0.15	0.13	0.11	0.05	0.13	0.09	0.22	0.43	–	0.03
Total	99.47	99.42	99.49	99.78	99.56	99.33	99.75	99.38	100.72	99.84	99.76
An, %	12.0	13.7	30.0	28.5	27.2	51.0	49.0	18.5	30.0	21.1	14.2

tion and divergence of these estimates, the average temperature of 620–650°C was evaluated for the eclogite-amphibolites and 640°C for the crystalline schists (Pattison and Newton, 1989).

According to the arrangement of isopleths of jadeite content in the diagram of Holland (1980), the stability of omphacite with *Jd* content up to 34% in the assemblage of *Cpx* + *Pl* + *Qtz* corresponds to a pressure of 12–12.5 kbar at $T = 650$°C. The *Hbl–Grt–Pl–Qtz* barometer (Kohn and Spear, 1990) cannot be used for eclogite-amphibolites, because it is developed for low-Na amphiboles with Na < 0.6 f.u., while this value is much higher in most amphiboles of eclogite-amphibolites. Medium-Na amphiboles are stable in the crystalline

Table 5. Microprobe analyses of minerals from clinopyroxene–plagioclase kelyphitic rims ($Cpx^2 + Pl^2$) around primary omphacitic clinopyroxene (Cpx^1)

Component	12						9/3					
	Cpx^1 ⟶	Cpx^2 +	Pl^2	Cpx^1 ⟶	Cpx^2 +	Pl^2	Cpx^1 ⟶	Cpx^2 +	Pl^2	Cpx^1 ⟶	Cpx^2 +	Pl^2
SiO_2	52.83	51.88	60.10	52.42	52.08	59.89	52.09	52.26	60.67	52.19	51.61	61.42
TiO_2	0.37	0.32		0.40	0.59	–	0.31	0.24	–	0.45	0.53	–
Al_2O_3	9.47	3.93	24.99	9.90	5.04	23.08	9.32	2.75	24.28	9.77	6.37	23.87
Fe_2O_3	4.05	2.88	–	1.46	4.38	–	5.14	1.43	–	2.93	3.99	–
FeO	1.60	3.71	–	4.38	1.44	–	1.47	5.65	–	3.32	2.44	–
MnO	–	–	–	0.08	0.04	–	–	0.06	–	–	0.11	–
MgO	10.21	13.61	–	9.92	12.75	–	10.12	13.37	–	9.65	11.74	–
CaO	16.78	22.22	6.52	18.34	22.04	6.76	16.98	23.15	5.84	17.11	20.50	5.37
Na_2O	4.66	1.16	8.01	3.62	1.34	7.95	4.54	0.70	8.72	4.31	2.58	9.05
K_2O	–	0.03	0.03	–	–	0.07	–	0.02	0.04	0.03	–	0.03
Total	99.97	99.73	99.65	100.39	99.83	97.75	99.97	99.63	99.95	99.76	99.85	99.74
Si	1.91	1.91		1.89	1.91		1.89	1.94		1.90	1.89	
Ti	0.01	0.01		0.01	0.02		0.01	0.01		0.01	0.01	
Al	0.40	0.17		0.42	0.22		0.40	0.12		0.42	0.28	
Fe^{3+}	0.11	0.08		0.04	0.04		0.14	0.04		0.08	0.11	
Fe^{2+}	0.05	0.11		0.13	0.14		0.04	0.18		0.10	0.07	
Mn	–	–		–	–		–	–		–	–	
Mg	0.55	0.75		0.54	0.70		0.55	0.74		0.52	0.64	
Ca	0.65	0.88		0.71	0.87		0.66	0.92		0.67	0.81	
Na	0.33	0.08		0.25	0.10		0.32	0.05		0.30	0.18	
K	–	–		–	–		–	–		–	–	
Jd	21.7	0.1		20.0	4.0		17.2	0.6		21.3	6.2	
Ac	11.1	8.1		4.0	4.0		14.1	4.0		8.1	11.2	
Aug	67.2	91.8		76.0	92.0		68.7	95.4		70.6	82.6	
$X_{Fe^{2+}}$	0.08	0.13		0.20	0.16		0.09	0.19		0.16	0.11	
An, %			31			32			27			25

schists, and the barometer of Kohn and Spear yielded a value of 11 kbar, which is close to the estimates of Holland (1980).

We assumed the following conditions of the prograde metamorphic stage for the eclogite-amphibolites and *Grt–Cpx–Hbl–Pl* crystalline schists of the Buchim Block: $T = 650°C$, $P = 12–12.5$ kbar, corresponding to a depth of 46–48 km and a geothermal gradient of 14°C/km. The relatively low content of the jadeite component in clinopyroxene of the eclogitic rocks (no higher than 25–34%) indicates that the Buchim Complex is a typical representative of the crustal eclogite facies of moderate depth. The obtained *P–T* estimates characterize the conditions of prograde metamorphism of the Buchim Block as a whole, because the eclogite-amphibolites, garnet–clinopyroxene–amphibole–plagioclase crystalline schists, and their host rocks are determined to be the products of the same metamorphic facies.

The following features are important for genetic interpretation of the reactional textures: (1) symplectites around omphacite grains contain extremely low-Na clinopyroxenes and have a cryptocrystalline texture; (2) garnet grains with $Hbl^2–Pl^2$ reaction rims preserve their prograde zoning even in the narrow outermost margins adjacent to the hornblende rims; (3) plagioclase in $Hbl^2–Pl^2$ rims on garnets are significantly more calcic than that in the groundmass.

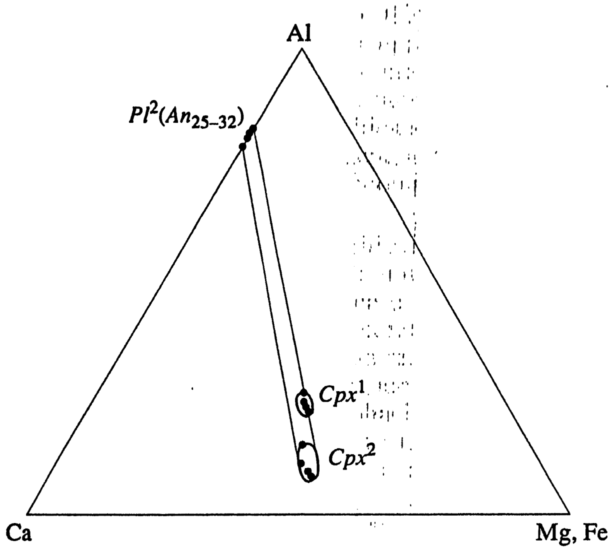

Fig. 6. Compositional relationships between primary omphacite (Cpx^1) and secondary Cpx^2 + Pl^2 assemblage in kelyphites.

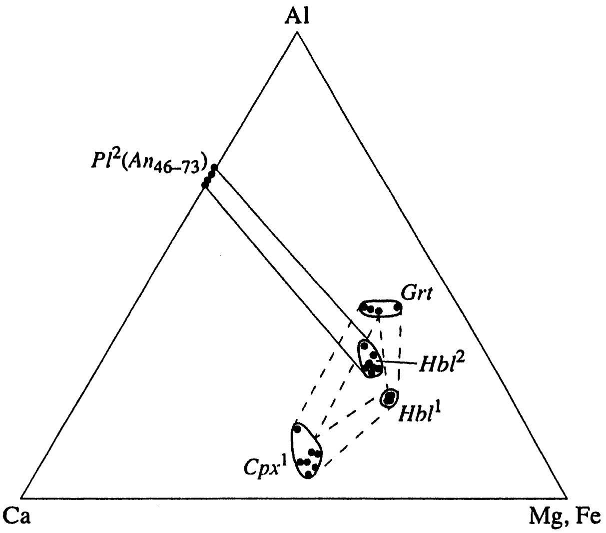

Fig. 7. Mineral compositions in the primary assemblage $Grt + Cpx^1 + Hbl^1$ and secondary Hbl^2 + Pl^2 kelyphites around the garnet at its contacts with Cpx^1 and Hbl^1.

The replacement of omphacite by the assemblage of low-Na clinopyroxene and sodic plagioclase is always considered a distinct indication of uplift and decompression (Cuthbert and Carswell, 1990; Joanny *et al.*, 1991; Hoinkes *et al.*, 1991; O'Brien, 1993; *Italian Eclogites* ..., 1993), because this secondary assemblage has much larger mole volume compared to omphacite. A very rapid uplift precludes the recrystallization of minerals and causes the cryptocrystalline texture of the kelyphitic rims. A wide gap in jadeite contents between the two clinopyroxene populations (25–34% *Jd* in the primary omphacite and 1–6% *Jd* in the augite from symplectites) most probably indicates that the reaction textures originated at the final uplift phase at a significantly shallower depth in comparison to the primary environment. It is evident from the fact that the symplectites do not contain *Cpx* of intermediate compositions that would mark the entire process of omphacite-bearing rock exhumation. It is more realistic to think that the uplift was catastrophically rapid, at a rate exceeding the rate of replacement, and no symplectites formed during each stage of decompression except the final one.

Some features of the kelyphitic rims around omphacite and garnet indicate that the uplift was not accompanied by a temperature decrease at its initial stages and occurred under isothermal conditions or even at an inertial increase of the temperature. These features are as follows: (a) augite crystallization instead of amphibole in symplectite after the omphacite, (b) the preservation of prograde zoning in the garnets in spite of their replacement with Hbl^2–Pl^2 rims and the occurrence of high-temperature hastingsite–pargasite amphibole in the rims, and (c) an abrupt increase in the *An* content of the plagioclase in these rims.

If our conclusions are true, and the temperature was really maintained at 650°C or even 700°C during the uplift, the content of 6% *Jd* in the symplectitic augite allows us to estimate the pressure at 4–4.5 kbar (14–16 km) during the kelyphitization by the *Cpx–Ab–Qtz* barometer (Holland, 1980). The Buchim Block probably was tectonically stabilized at this depth and kelyphitization began.

The later, rather poor alteration of the metabasites displays retrograde features and comprises the replacement of the clinopyroxene and hastingsite–pargasite hornblende by pale green amphibole, the development of secondary epidote, and the albitization of the plagioclase.

STABILITY OF SODIC PLAGIOCLASE IN ECLOGITES UNDER ECLOGITIC FACIES CONDITIONS OF MODERATE DEPTH (EXEMPLIFIED BY THE ROCKS OF THE BUCHIM BLOCK)

Almost all samples of eclogites and eclogite-amphibolites of the Buchim Block contain sodic primary plagioclase, which is not typical of rocks of this group.

There are two reasons why albite (oligoclase) is absent from crustal eclogites, which are normally classified as plagioclase-free rocks. Albite could either be unstable in any rock or be absent as a result of a specific bulk rock composition. However, albite-oligoclase is stable throughout a significant part of the eclogitic facies (Carswell, 1990). Albite becomes unstable only at pressures above the *Jd* + *Qtz* = *Ab* equilibrium (Holland, 1980), i.e., at pressures >14–18 kbar depending on the temperature.

Under conditions typical of most crustal eclogitic complexes (P < 14–18 kbar and T = 500–700°C), albite

Table 6. Representative microprobe analyses of minerals from amphibole–plagioclase ($Hbl^2 + Pl^2$) kelyphitic rims between garnet and primary clinopyroxene (amphibole)

Component	6				26E				6/2		9/3		21	12
	$Hbl^2 + Pl^2$		$Hbl^2 + Pl^2$		$Hbl^2 + Pl^2$		$Hbl^2 + Pl^2$		$Hbl^2 + Pl^2$		$Hbl^2 + Pl^2$		Hbl^2	Hbl^2
SiO_2	39.79	50.53	39.91	52.30	39.07	51.25	38.28	51.20	41.76	56.50	38.97	49.32	42.20	38.35
TiO_2	0.32	–	0.10	–	0.21	–	0.22	–	0.36	–	–	–	0.35	0.07
Al_2O_3	17.24	32.00	17.08	30.57	18.97	32.04	18.91	31.06	15.77	27.19	21.49	32.11	12.78	19.89
FeO	15.44		15.25	–	15.43	–	14.69	–	16.56	–	12.32	–	22.62	14.20
MnO	0.26	–	0.21	–	0.15	–	0.29	–	0.23	–	0.21	–	0.16	0.20
MgO	10.56	–	10.64	–	9.51	–	10.69	–	8.76	–	10.52	–	6.65	10.13
CaO	10.95	13.35	11.32	12.19	11.11	12.87	11.05	13.27	11.92	9.58	10.70	14.85	10.72	10.60
Na_2O	2.37	3.49	2.26	4.46	3.19	3.21	3.76	4.12	1.56	6.11	3.40	3.05	1.61	3.37
K_2O	0.69	0.05	0.84	0.06	0.06	–	0.08	0.01	1.02	0.20	0.09	0.04	1.09	0.38
Total	97.62	99.42	97.61	99.58	97.70	99.37	97.97	99.66	97.94	99.58	97.70	99.37	98.18	97.19
Si	5.80		5.83		5.72		5.58		6.19		5.60		6.35	5.60
Al(IV)	2.20		2.17		2.28		2.42		1.81		2.40		1.65	2.40
Al(VI)	0.76		0.77		1.00		0.83		0.95		1.24		0.61	1.03
Ti	0.04		0.01		0.02		0.02		0.04		–		0.04	0.01
Fe^{3+}	1.15		1.05		0.83		1.01		0.36		0.90		0.83	1.01
Fe^{2+}	0.73		0.81		1.05		0.78		0.36		0.90		0.83	1.01
Mn	0.03		0.03		0.03		0.04		0.03		0.03		0.02	0.02
Mg	2.29		2.34		2.07		2.32		1.93		2.25		1.49	2.21
Ca	1.71		1.77		1.74		1.73		1.89		1.65		1.73	1.66
Na	0.67		0.64		0.91		1.06		0.45		0.95		0.47	0.95
K	0.13		0.16		0.01		0.01		0.19		0.02		0.21	0.07
$X_{Fe\ tot}$	0.45		0.45		0.48		0.44		0.52		0.40		0.66	0.44
Na_B	0.26		0.20		0.24		0.24		0.08		0.33		0.25	0.32
$(Na + K)_A$	0.76		0.59		0.68		0.84		0.56		0.64		0.61	1.03
An, %		68		60		69		67		46		73		

and oligoclase are common in various mineral assemblages. For example, albite is usual in blueschists, omphacite–garnet–hornblende amphibolites, and gneisses that associate with eclogites. Oligoclase often occurs in mica gneisses that alternate with eclogites and crystallized under similar *P–T* conditions (Klemd *et al.*, 1991).

Albite–oligoclase was often detected as an equilibrium phase in many eclogitic rocks with garnet and omphacite (Velilla and Hach-Ali, 1986; Heinrich, 1986; El-Shazly *et al.*, 1990; Ghent *et al.*, 1987; Schulz, 1993). These eclogites always correspond to moderate-depth kyanite-free varieties, whose omphacite contains <35–43% *Jd*. Using the term "eclogite" in its strict sense, geologists classify these plagioclase-bearing rocks either with omphacite–albite–garnet amphibolites (Heinrich, 1986) or eclogite-amphibolites (Schulz, 1993). However, this is a merely terminological problem as these rocks can be also termed as plagioclase-bearing eclogites. In any event, it is obvious that there is a certain *P–T* interval within the eclogite facies ($P = 10–16$ kbar, $T = 500–700°C$) over which albite and oligoclase are stable both in eclogites and associated silicic rocks, and the absence or presence of these minerals are controlled only by the bulk rock composition.

Let us consider the problem of sodic plagioclase occurrence in crustal eclogite complexes of moderate depth using the example of the Buchim Block. The compositions of minerals in eclogitic rocks of the Buchim Block, including a wide series of clinopyroxene solid solutions *Aug*–Na-*Aug*–*Omp* ($Jd \leq 34\%$), are plotted in a Na–Al–(Mg, Fe) diagram (Fig. 8) to illustrate a simplified model for equilibria between *Cpx*, *Grt*, *Ab*(*Olg*), and *Qtz*. The diagram demonstrates that the albite-free Cpx_{Na-Ca} ($Jd < 34\%$) + *Grt* assemblage, in which oligoclase is absent or occurs as an accessory mineral, is stable in rocks poor in Na and Al (generalized type 1). The $Cpx_{Na-Ca} + Grt + Ab(Olg)$ assemblage, typical of eclogitic rocks of the Buchim Block, should occur in rocks with higher Na and Al (generalized type 2).

Table 7. Microprobe analyses of a garnet grain with inclusions of primary hornblende and clinopyroxene along a profile across the grain from its core to rim (Sample 9/3)

Component	*Grt*	*Hbl*[1]	*Grt*	*Hbl*[1]	*Grt*	*Gpx*[1]	*Grt*	*Hbl*[1]
	core		transitional zone		near the rim		rim	groundmass
SiO_2	38.58	41.37	38.17	40.92	38.54	51.80	39.22	42.23
TiO_2	–	1.33	0.09	1.28	–	0.44	–	1.74
Al_2O_3	21.95	18.31	21.85	18.54	22.34	9.13	22.04	14.98
Fe_2O_3						4.02		
FeO	22.48	11.49	22.44	12.03	21.92	2.35	21.05	12.31
MnO	0.57	0.01	0.59	–	0.67	0.13	0.45	0.05
MgO	6.69	11.99	6.63	11.30	7.07	10.59	7.85	12.36
CaO	9.71	9.86	9.98	10.45	9.41	17.36	9.32	10.57
Na_2O	–	3.32	–	2.95	–	3.85	–	3.34
K_2O	–	0.58	–	0.62	–	–	–	0.60
Total	99.98	98.26	99.75	98.09	99.95	99.87	99.93	98.18
Si		5.88		5.87		1.88		6.11
Ti		0.14		0.14		0.01		0.19
Al		3.07		3.13		0.39		2.55
Fe^{3+}		0.86		0.70		0.11		0.54
Fe^{2+}		0.51		0.74		0.07		0.95
Mn		–		–		–		0.01
Mg		2.54		2.42		0.57		2.66
Ca		1.50		1.61		0.68		1.64
Na		0.91		0.82		0.27		0.94
K		0.11		0.11		–		0.11
X_{Fe}	0.65	0.35	0.66	0.37	0.63	0.12	0.60	0.36
Alm	47.5		47.1		46.4	*Jd* 16	44.4	
Sps	1.2		1.3		1.4	*Acm* 11	1.0	
Prp	25.1		24.8		26.6	*Aug* 73	29.5	
Grs	26.2		26.8		25.6		25.1	
Na_B		0.50		0.39				0.36
$(Na + K)_A$		0.52		0.54				0.69

Indeed, plagioclase-bearing and rare plagioclase-free rocks exist within the same eclogitic bodies. This fact can be related only to variations in rock compositions, namely to their various (Mg + Fe)/(Na + Al) ratios. The variations in Ca : Al : (Mg, Fe) in the metabasites (Fig. 5) cause the association of the Buchim eclogites with garnet, pyroxene, and ordinary amphibolites, crystalline schists, and gneisses, in which plagioclase stability is not restricted. The stability of sodic plagioclase is also not constrained in the associated mica and kyanite–garnet gneisses and metapelites, which are rocks rich in Na and Al. Therefore, the phase relations shown in Figs. 5 and 8 indicate that the proper plagioclase-free *Grt–Cpx–(±Hbl, Czo, Rt)–Qtz* crustal eclogites that are very rare in the Buchim Block could originate only after metabasites of specific composition with high (Ca + Al)/(Mg + Fe) and low (Na + Al)/(Mg + Fe) ratios. The other eclogites can contain sodic plagioclase.

Eclogite-bearing complexes of moderate depths similar to the Buchim Block that formed at $T = 500$–700°C and P from 9–10 to 17 kbar and that contain eclogites in the strict sense (plagioclase-free rocks) in association with albite(oligoclase)–omphacite–garnet–quartz eclogitic rocks can be classified with the *subfacies of plagioclase eclogites* recognizing the fact that the absence or presence of plagioclase in these rocks are controlled only by metabasite composition.

In the assemblages considered above, an increase in the pressure causes enrichment of the clinopyroxene in the jadeite component accompanied by a decrease in albite (oligoclase) amount in the rock, i.e., the Cpx_{Na-Ca} + *Grt* field in Fig. 8 expands, and the Cpx_{Na-Ca} + *Ab*(*Olg*) + *Grt* field becomes smaller. Under pressures corresponding to the stability of *Cpx* with 40–43% *Jd*, the monovariant reaction *Grt* + *Ab* ⟶ *Cpx* (>43% *Jd*) + *Ky* and the transition to a deeper *subfacies of kyanite eclogites* occur.

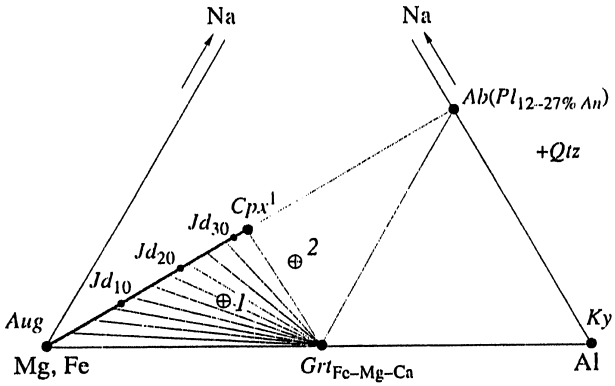

Fig. 8. Principal equilibria of primary clinopyroxene with garnet and primary sodic plagioclase in a Na–Al–(Mg, Fe) diagram in eclogite-amphibolites of the Buchim Block as an example of mineral assemblages of the moderate-depth plagioclase subfacies of crustal eclogites.
Bulk rock compositions: (*1*) poor in Na and Al (Cpx_{Ca-Na} + *Grt* assemblage, *Pl* is absent), (*2*) rich in Na and Al (Cpx_{Ca-Na} + *Grt* + *Pl* assemblage).

In this facies, albite (oligoclase) survives only in garnet-free rocks, for example, in omphacite–albite–amphibole–quartz schists and amphibolites (Cpx_{Na-Ca} + *Ab* assemblage in Fig. 8) and cannot crystallize in *Cpx* + *Grt* assemblage at any rock composition. Simultaneously, kyanite becomes a usual mineral of eclogites.

Table 8. Garnet–clinopyroxene thermometry of the prograde metamorphic stage

Component	Coexisting minerals and their iron numbers	*Grt–Cpx*[1] thermometer				
		Sch.	E.G.	K.	S.	P.N.
	Weakly altered eclogite-amphibolites					
9E	Grt_{58}–Cpx_{19}	640	713	647		
	Grt_{59}–Cpx_{15}	574	640	560		
	Grt_{58}–Cpx_{13}	600	676	602		
9/2	Grt_{59}–Cpx_{16}	640	663	609		
	Highly amphibolized eclogite-amphibolites					
26E	Grt_{63}–Cpx_{15}	583	690	651		
	Grt_{63}–Cpx_{17}	648	726	691		
12	Grt_{55}–Cpx_{8}	575	600	583		
9/3	Grt_{63}–Cpx_{12} (inclusions in *Grt* rim)	630	595	544		
	***Grt–Cpx–Hbl–Pl* crystalline schists with low-Na *Cpx*[1]**					
6	Grt_{61}–Cpx_{15}				745	640

Note: *Grt–Cpx* thermometers for crustal eclogites: Sch. (Schliestedt, 1986), E.G. (Ellis and Green, 1979), K. (Krogh, 1988). *Grt–Cpx* thermometers for garnet–clinopyroxene crystalline schists: S. (Sengupta *et al.*, 1989), P.N. (Pattison and Newton, 1989). The latter thermometer is not applicable to *Cpx* with $Na_2O > 2.2$ wt % and *Grt* with $X_{Mg} < 0.125$.

Finally, if the pressure increases above the conditions of the *Ab* = *Jd* + *Qtz* reaction, albite disappears both in metabasites and silicic gneisses, and gradual transition to subfacies of *jadeitic*, coesitic, and *diamond-bearing eclogites* occurs.

SPECIFIC FEATURES OF ECLOGITE-AMPHIBOLITES COMPOSING SHEET-SHAPED BODIES WITHIN THE BUCHIM BLOCK OF THE SERBO–MACEDONIAN MASSIF

The eclogites and eclogite-amphibolites do not show evidence of metamorphic differentiation, silica–alkaline metasomatism, or migmatization. Thus, we can estimate some chemical features of the protoliths of these metabasites using low-mobile elements (Ti, Y, REE, Hf, Cr, Ni, Sc, and some others). Major, trace, and rare earth elements were determined in nine representative samples from three eclogite bodies (Samples 9, 10, 11 in Tables 9, 10).

The eclogite-amphibolites, like most crustal eclogites of the crystalline basement of the Mediterranean Belt and central Europe, correspond to low-K basalts (K_2O < 1 wt %), which are significantly evolved (*MGN* < 0.6) relative to the primary mantle melts. According to the (Na_2O + K_2O)/SiO_2 ratio (Le Bas *et al.*, 1986), we distinguish two main groups (series) among the metabasites: (a) tholeiitic and (b) subalkaline with small amounts of normative nepheline (<5%). Each of the three eclogitic bodies has specific compositional features (Figs. 9, 10, 11). The eclogite-amphibolites of body 9 are typical representatives of the tholeiitic group, which are comparable with highly magnesian low potassic slightly evolved tholeiitic basalts and have *MGN* = 0.58–0.50. The metabasites are close to MORB in some incompatible (Zr, Hf, Y, Nb, REE) and compatible (Cr, Ni, Co, Sc) trace element concentrations (Tables 9, 10). The fractionation of basalts within body 9 causes a decrease in MgO (9.11–7.33 wt %), increase in FeO (11.7–12.9 wt %), TiO_2 (1.26–2.01 wt %), and P_2O_5 (0.12–0.21 wt %). The contents of HFSE and REE increase, and the concentrations of iron-group elements (Cr, Ni, Co) decrease with decreasing MgO. The alkali and alkali-earth elements (K, and particularly Ba and Sr) do not show a good correlation with major elements and possibly were mobile during retrograde metamorphism (these features are typical of all eclogitic bodies in question and are not considered hereafter). Some specific ratios of low-mobile elements are as follows: $(La/Sm)_n = 0.83 \pm 0.10$, $(La/Yb)_n = 0.65 \pm 0.12$, $(Sm/Yb)_n = 0.78 \pm 0.08$, $La/Nb = 1.58 \pm 0.36$, $Y/Nb = 11.67 \pm 6.4$, $Ti/Y = 284 \pm 14$. They are independent of the melt fractionation and are close to these ratios in N-MORB (Schilling *et al.*, 1983; Le Roex, 1987; Sun and McDonough, 1989). All metabasites of body 9, however, have low Zr concentrations, which are poorly fractionated (Zr = 32 ± 5.6 ppm) in comparison to the other incompatible elements. Hence, the metabasites of eclogite-amphibo-

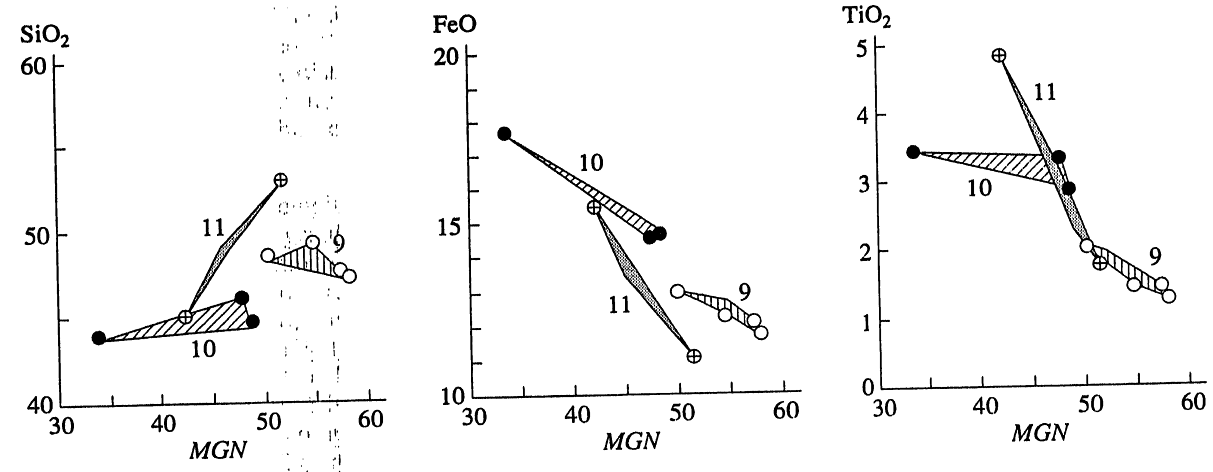

Fig. 9. Variation of SiO_2, FeO, and TiO_2 with *MGN* in eclogite-amphibolites of the Buchim Block (Samples 9, 10, 11).

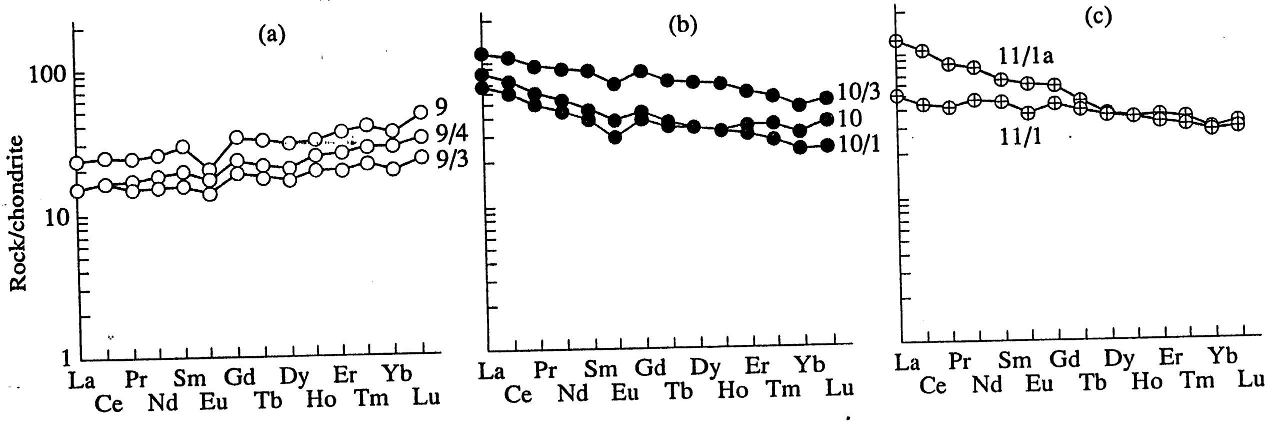

Fig. 10. Rare-earth element patterns for the most magnesian eclogite-amphibolites of the Buchim Block. Sample numbers are shown near the curves. Chondrite composition is after Sun and McDonough (1989).

litic body 9 show a distinct behavior of Zr and REE (Zr*/Zr = 0.59 ± 0.27). The similarity between these metabasites (body 9) and N-MORB, their relative depletion in LREE, and the distinct negative Zr and less pronounced Hf anomalies are well illustrated by the most magnesian rock of this series (Sample 9, *MGN* = 0.58, Figs. 10a, 11a).

The metabasites of eclogite-amphibolite body 10 represent the second rock group comprising low-potassic basalts that are transitional between tholeiitic and subalkaline varieties and are significantly evolved (*MGN* = 0.49–0.34, Table 8). The metabasites of body 10 are generally lower in SiO_2 (44.96 ± 1.1 wt %) and CaO (10.23 ± 0.64 wt %), higher in TiO_2 (3.20 ± 0.31 wt %) and K_2O (0.19 ± 0.01 wt %), and richer in Nb (12 ± 2.7 ppm) in comparison to the eclogite-amphibolites of body 9. The part of the body that is primarily most evolved (Sample 10/3) has higher contents of FeO, P_2O_5, HFSE, REE and much lower abundances of Cr, Ni, and Co (Table 9). The enrichment in TiO_2 with increasing Fe contents in these rocks is less distinct than that of the tholeiitic metabasites of body 9. The relative enrichment of the eclogite-amphibolite of body 10 in incompatible elements in comparison with N-MORB is well illustrated by trace-element patterns (Figs. 10b, 11b) and some indicative ratios: $(La/Sm)_n$ = 1.56 ± 0.39, $(La/Yb)_n$ = 2.51 ± 0.97, $(Sm/Yb)_n$ = 1.59 ± 0.33, La/Nb = 1.55 ± 0.41, Y/Yb = 3.29 ± 0.74, Ti/Y = 515 ± 140. According to these chemical features, the basaltic series of body 10 can be affiliated with basalts of the enriched type from oceanic spreading zones (T-MORB), which is transitional between N-MORB and oceanic island basalts. The latter are the most enriched in incompatible elements. In contrast to the ratios mentioned above, the Zr contents (39 ± 4.4 ppm) of the eclogite–amphibolites in body 10 are significantly lower than those of oceanic basalts of the subalkaline type, and are rather uniform. These chemical features are demonstrated in Fig 11b for the most magnesian basalt 10/1 (*MGN* = 0.49) of body 10, which has

Table 9. Contents of major (wt %) and trace (ppm) elements in eclogite-amphibolite bodies

Component	9	9/3	9/4	9/5	10	10/1	10/3	11/1	11/1a
SiO_2	47.30	49.27	48.55	47.59	46.16	44.74	43.98	45.06	52.94
TiO_2	1.26	1.43	2.01	1.42	3.31	2.85	3.43	4.83	1.75
Al_2O_3	14.39	14.31	14.11	14.97	14.87	16.35	13.60	13.71	13.53
FeO	11.69	12.22	12.91	12.01	14.52	14.61	17.69	15.41	11.03
MnO	0.19	0.16	0.17	0.18	0.28	0.27	0.32	0.28	0.23
MgO	9.11	8.29	7.33	9.09	7.44	7.76	5.05	6.32	6.59
CaO	12.86	10.53	12.01	12.04	9.97	9.85	10.97	10.03	9.72
Na_2O	3.06	3.57	2.62	2.50	2.85	2.93	3.66	3.61	3.80
K_2O	0.03	0.06	0.08	0.10	0.18	0.19	0.20	0.44	0.23
P_2O_5	0.12	0.15	0.21	0.10	0.41	0.44	1.10	0.29	0.16
LOI	0.70	0.25	0.85	0.15	0.05	0.85	0.25	0.95	0.50
Total	100.71	100.24	100.85	100.15	100.04	100.84	100.25	100.93	100.48
MGN	0.58	0.55	0.50	0.57	0.48	0.49	0.34	0.42	0.52
Sr	99	75	210	132	104	105	131	92	59
Sc	45	37	45	40	46	33	41	49	38
Cr	373	165	133	208	138	207	10	114	246
Ni	112	83	71	100	47	128	27	64	115
Co	51	40	45	44	43	53	23	46	33
Zr	34	39	28	27	34	42	41	26	57
Y	28	29	42	20	52	34	82	44	62
Nb	3	2	3	3	11	10	15	10	12

Note: The rocks were analyzed at the Vernadsky Institute of Geodemistry and Analytical Chemistry, Russ. Acad. Sci. (GEOKhI RAS) by XRF (major elements, analyst T. Romasheva) and ICP (trace elements, T.V. Shumskaya and L.N. Bannykh). Nb was analyzed by XRF at the Institute of the Geology of Ore Deposits, Petrography, Mineralogy, and Geochemistry, Russ. Akad. Sci. (IGEM RAS) (analyst T.M. Marchenko).

Table 10. Contents (ppm) of rare-earth elements and Hf in eclogite-amphibolite bodies

Element	9	9/3	9/4	9/5	10	10/1	10/3	11/1	11/1a
La	3.5	3.5	5.5	1.5	16.0	20.0	28.0	12.0	30.0
Ce	10.0	10.0	15.0	3.5	37.0	45.0	68.0	27.0	65.0
Pr	1.4	1.6	2.3	0.5	4.8	5.8	9.0	4.0	8.0
Nd	7.1	8.5	12.0	2.4	21.0	25.0	42.0	22.0	37.0
Sm	2.4	3.0	4.5	0.7	6.0	7.0	13.0	7.0	10.0
Eu	0.8	1.0	1.2	1.0	1.7	2.2	4.0	2.2	3.5
Gd	4.0	4.8	7.0	1.1	8.0	9.0	17.0	9.0	12.0
Tb	0.67	0.81	1.20	0.20	1.30	1.40	2.70	1.50	1.70
Dy	4.3	5.2	7.8	1.5	8.5	8.5	1.6	9.2	9.5
Ho	1.10	1.40	1.80	0.42	1.80	1.80	3.80	2.00	2.00
Er	3.2	4.3	6.0	1.4	5.7	5.0	9.8	6.0	5.5
Tm	0.55	0.71	1.00	0.28	0.90	0.70	1.40	0.90	0.80
Yb	3.3	4.8	6.0	1.7	5.2	4.0	8.0	5.0	4.8
Lu	0.60	0.82	1.20	0.42	0.92	0.61	1.30	0.82	0.75
Hf	1.3	2.2	2.7	1.2	4.2	4.0	8.0	3.2	6.9

Note: The rocks were analyzed at GEOKHI RAS by INAA (analyst G.M. Kolesov).

distinct negative Zr [$(Zr^*/Zr)_n = 0.24$] and Nb anomalies [$(Nb^*/Nb)_n = 0.61$].

The metabasites of sheet-shaped eclogitic body 11 also correspond to low-K basalts, although their K_2O content is somewhat higher ($K_2O = 0.23$–0.44 wt %) than in the rocks of body 10. The metabasites of body 11 are the least magnesian ($MgO = 6.46 \pm 0.19$ wt %), aluminous ($Al_2O_3 = 13.62 \pm 0.13$ wt %), and calcic ($CaO = 9.88 \pm 0.22$ wt %) among the studied eclogitic rocks of the Buchim Block. They also apparently belong to group 2 of enriched subalkaline basalts similar to T-MORB, a fact also illustrated by the indicative ratios $(La/Sm)_n = 1.94$, $(La/Yb)_n = 4.48$, $(Sm/Yb)_n = 2.31$, La/Nb = 2.5, Y/Nb = 5.16 and incompatible-element patterns in Sample 11/1a (Figs. 10, 11). The latter pattern has a distinct asymmetry with an enrichment in elements with low K_D and distinct negative anomalies of Nb [$(Nb^*/Nb)_n = 0.49$], Zr [$(Zr^*/Zr)_n = 0.21$], and Ti [$(Ti^*/Ti)_n = 0.57$]. The metabasalt of Sample 11/1a is more enriched in incompatible elements in comparison with the other sample from this body but has higher MgO, lower FeO, and significantly lower SiO_2 contents. These features do not agree with the normal trend of fractional crystallization in basaltic melts. The composition of Sample 11/1 can be produced by the fractionation of 2–3% titanomagnetite from the composition of Sample 11/1a. This model agrees with variations in the contents of incompatible elements and their indicative ratios.

The variations of major- and trace-element concentrations within each individual eclogite body of the Buchim Block are small and their distribution agrees with the fractionation model for the MORB-type series (Sobolev *et al.*, 1988; Dmitriev *et al.*, 1990; Zakariadze *et al.*, 1993 and references therein). The diversity between the incompatible-element concentrations in different metabasite bodies is larger and is likely to be related to the compositions of the primary high-magnesian magmas. The compositions of rocks that are comparable with N-MORB (body 9), and T-MORB (bodies 10, 11) are most dissimilar. These differences are most distinct in the La/Nb, Zr/Nb, Y/Nb, La/Sm, La/Yb ratios, and the values of negative HFSE anomalies. According to many publications (Le Roex, 1987; Johnson *et al.*, 1990; Hauri and Hart, 1994), these ratios and values do not change during the generation of primary high-magnesian magmas in the mantle at melting degree >10% or during the magma differentiation. Thus, these values could be also considered to be geochemical indicators of the mantle magma sources. Among these values, the negative Zr anomalies, which are typical of both metabasite types, are the most distinct. It has long been hypothesized that negative HFSE anomalies occur only in rocks originated in the mantle wedge above subduction zones (Ringwood, 1975; Tatsumi *et al.*, 1986; Hofmann *et al.*, 1988). However, there is convincing evidence that negative HFSE anomalies also occur in suboceanic and subcontinental mantle domains, *inter alia* in zones of oceanic spreading and intra-plate hot spot areas. The generation of HFSE anomalies is believed to be related to the percolation of highly magnesian magmas through mantle peridotites (Salters and Shimizu, 1988; Hauti and Hart, 1994; Johnson, 1990). Thus, we would not consider the negative HFSE anomalies in metabasites of the Buchim Block as indicators of their primary magma generation above subduction zones. The HFSE and REE partition in these zones is usually accompanied by a significant decrease in the contents of medium and heavy rare-earth elements, Cr, and Ni in comparison to their concentrations in MORB series (Pearce, 1983; Kelemen *et al.*, 1993). However, these specific chemical features are absent in the metabasites (Fig. 11a), which also do not show any depletion in iron-group elements.

It is important to correlate these geochemical data with geological observations. According to the latter, the studied metabasite bodies are interpreted as hypabyssal sheet-shaped intrusions in the continental crust. Intrusions of this composition are abundant within the crystalline basement of the Mediterranean Mobile Belt, for example, in the eastern Alps (Thoeni and Jagoutz, 1992) and Rhodopean Massif (Zakariadze *et al.*, 1993). It is difficult to interprete the geodynamic setting of these intrusions. They probably mark the embryonal phases of paleospreading at the initial stages of a tectonic cycle typical of the Mediterranean (from Panafrican to Alpian), and, thus, represent early portions of oceanic-type magmas emplaced into the thinned continental crust or sedimentary sequences, which occupied restricted areas on the young oceanic crust.

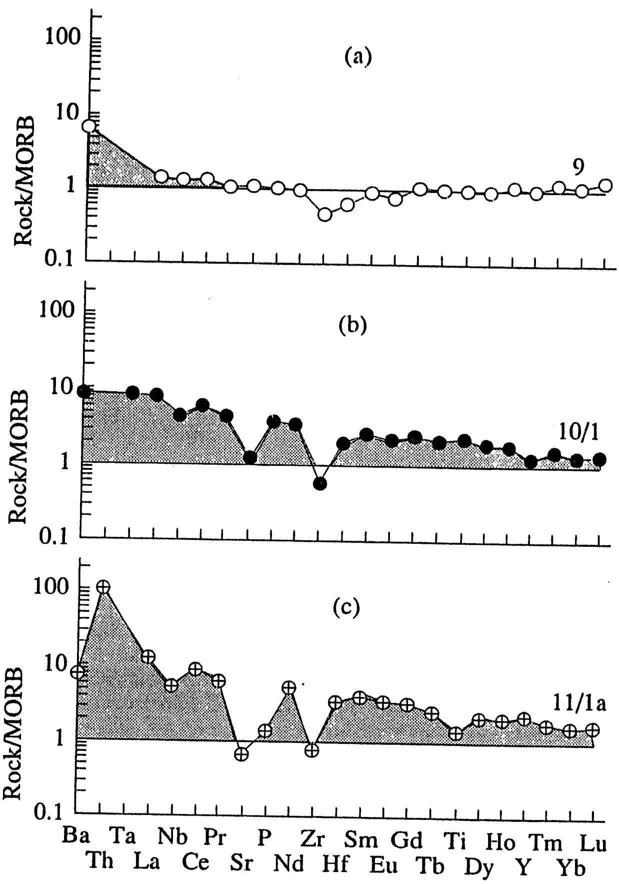

Fig. 11. Incompatible-element patterns for the most magnesian eclogite-amphibolites of the Buchim Block.
Sample numbers are shown near the curves. The hatched areas denote elements enriched relative to average N-MORB (Sun and McDonough, 1989).

CONCLUSION

(1) Prograde equilibria are studied in the plagioclase-bearing eclogitic rocks and clinopyroxene–garnet–amphibole–plagioclase crystalline schists of the Buchim Block of the Serbo–Macedonian Massif. The following minerals are stable there: clinopyroxene of the *Aug*–Na-*Aug*–*Omp* series with a *Jd* content up to 34%, garnet with a distinct prograde zoning (up to 35% *Prp* in marginal zones), hastingsite–tschermakite–pargasite amphibole, and primary oligoclase. The Na content in the coexisting *Cpx* and *Pl,* the existence or

absence of *Pl, Hbl, Cpx*, and *Grt* in the metabasites, and the transition of the eclogites to eclogite-amphibolites, garnet and clinopyroxene amphibolites, and crystalline schists are controlled only by the Na/Al, (Na + Al)/(Mg + Fe), Ca : Al : (Mg, Fe) ratios of the rocks.

(2) According to mineralogical thermobarometry, the conditions of the prograde stage are as follows: $T = 650°C$, $P = 12–12.5$ kbar.

(3) The Cpx^2–Pl^2 symplectites around omphacite grains and Hbl^2–Pl^2 rims on the garnet at its contact with Cpx^1 and Hbl^1 originated during uplift. Some mineralogical features are indicative of very rapid uplift under the isothermal conditions or even at temperature increase, as well as of formation of reactional textures only at the end of the uplift during the stabilization of the geoblock at depth of 14–16 km.

(4) Some principal equilibria under conditions of the moderate-depth plagioclase subfacies of the eclogite facies ($P = 10–17$ kbar, $T = 500–700°C$) can be illustrated by the example of the eclogite-amphibolites of the Buchim Block. Under these conditions, plagioclase presence or absence in these rocks are controlled only by the rock composition.

(5) The protolith of the eclogite-amphibolites of the Buchim Block corresponds to basalts of oceanic spreading zones (N-MORB and T-MORB). Apparently, they were emplaced at the initial stages of paleospreading, when the earlier portions of oceanic-type magmas intruded into the thinned continental crust or sedimentary sequence on the young oceanic crust.

ACKNOWLEDGMENTS

The study was supported by the Russian Foundation for Basic Research (project nos. 96-05-64977 and 95-05-15479).

REFERENCES

Carswell, D.A., Eclogites and the Eclogite Facies: Definition and Classification, *Eclogite Facies Rocks*, Carswell, D.A., Ed., Glasgow: Blackie, 1990, pp. 1–13.

Cuthbert, S.J. and Carswell, D.A., Formation and Exhumation of Medium-Temperature Eclogites in the Scandinavian Caledonides, *Eclogite Facies Rocks*, Carswell, D.A., Ed., Glasgow: Blackie, 1990, pp. 180–203.

Dmitriev, L.V., Sobolev, A.V., Reisner, M.G., *et al.*, Petrochemical Groups of MORB Quench Glasses and Their Distribution in the Atlantic and Pacific Oceans, in *Magmatizm i tektonika okeana* (Ocean Magmatism and Tectonics), Moscow: Nauka, 1990, pp. 43–108.

Ellis, D.J. and Green, D.H., An Experimental Study of the Effect of Ca upon Garnet–Clinopyroxene Fe–Mg Equilibria, *Contrib. Mineral. Petrol.*, 1979, vol. 71, no. 1, pp. 13–22.

El-Shazly, A.K., Coleman, R.G., and Liou, J.G., Eclogites and Blueschists from Northeastern Oman: Petrology and *P–T* Evolution, *J. Petrol.*, 1990, vol. 31, no. 3, pp. 629–666.

Ghent, E.D., Black, P.M., Brothers, R.N., and Stout, M.Z., Eclogites and Associated Albite–Epidote–Garnet Paragneisses between Yamble and Cape Colnett, New Caledonia, *J. Petrol.*, 1987, vol. 29, no. 4, pp. 627–643.

Hauri, E.H. and Hart, S.R., Constraints on Melt Migration from Mantle Plumes: A Trace Element Study of Peridotite Xenoliths from Savai'i, Western Samoa, *J. Geophys. Res.*, 1994, vol. 99, no. B12, pp. 301–324.

Heinrich, C.A., Eclogite Facies Regional Metamorphism of Hydrous Mafic Rocks in the Central Alpine Adula Nappe, *J. Petrol.*, 1986, vol. 27, no. 1, pp. 123–154.

Hofmann, A.W., Chemical Differentiation of the Earth: Relationship between Mantle, Continental Crust and Oceanic Crust, *Earth Planet. Sci. Lett.*, 1988, vol. 90, pp. 297–314.

Hoinkes, G., Kostner, A., and Thoni, M., Petrologic Constraints for Eoalpine Eclogite Facies Metamorphism in the Austroalpine Otztal Basement, *Mineral. Petrol.*, 1991, vol. 3, pp. 237–254.

Holland, T.J.B., The Reaction Albite = Jadeite + Quartz Determined Experimentally in the Range 600–1200°C, *Am. Mineral.*, 1980, vol. 65, pp. 129–134.

Italian Eclogites and Related Rocks, Morten, L., Ed., Accad. Nazion. delle Scienze. D. XL Scritte e documenti. XI, 1993, pp. 1–275.

Joanny, V., Van Roermund, H., and Lardeaux J.M., The Clinopyroxene/Plagioclase Symplectite in Retrograde Eclogites: A Potencial Geothermobarometer, *Geol. Rundschau*, 1991, vol. 80, no. 2, pp. 303–320.

Johnson, K.T.M., Dick, H.J.B., and Shimizu, N., Melting of Oceanic Upper Mantle: An Ion Microprobe Study of Diopsides in Abyssal Peridotites, *J. Geophys. Res.*, 1990, vol. 95, no. B3, pp. 2661–2678.

Karamata, St. and Krstič, B., Terranes of Serbia and Neighbouring Areas, *Terraines of Serbia*, Knezevic, V. and Krstič, B., Eds., Belgrade, 1996, pp. 25–40.

Kelemen, P.B., Shimizu, N., and Dunn, T., Relative Depletion of Niobium in Some Arc Magmas and the Continental Crust: Partitioning of K, Nb, La, and Ce during Melt/Rock Reaction in Upper Mantle, *Earth Planet. Sci. Lett.*, 1993, vol. 120, pp. 111–134.

Klemd, R., Matthes, S., and Okrusch, M., High-Pressure Relics in Meta-Sediments Intercalated with the Weissenstein Eclogite, Munchberg Gneiss Complex, Bavaria, *Contrib. Mineral. Petrol.*, 1991, vol. 107, pp. 328–342.

Kohn, M.Y. and Spear, F.S., Two New Geobarometers for Garnet Amphibolites, with Application to Southeastern Vermont, *Am. Mineral.*, 1990, vol. 75, no. 1/2, pp. 89–96.

Krogh, E.J., The Garnet–Clinopyroxene Fe–Mg Geobarometer: A Reinterpretation of Existing Experimental Data, *Contrib. Mineral. Petrol.*, 1978, vol. 99, no. 1, pp. 44–48.

Le Bas, M.G., Le Maitre, R.W., Streckeisen, A., *et al.*, Chemical Classification of Volcanic Rocks Based on Total Alkali–Silica Diagram, *J. Petrol.*, 1986, vol. 27, no. 3, pp. 745–750.

Le Roex, A.P. Source Regions of Mid-Ocean Ridge Basalts: Evidence for Enrichment Processes, in *Mantle Metasomatism*, London: Academic, 1987, pp. 389–422.

Mirčovski, V., Petrographic and Petrological Features of the Eclogites from the Vicinity of the Kočevo Village, Northern Part of the Buchim Block, Macedonia, *Geol. Macedonica*, 1991, vol. 5, pp. 87–104.

O'Brien, P.J., Partially Retrograded Eclogites of the Minchberg Massif, Germany: Records of a Multi-Stage Variscan

Uplift History in Bohemian Massif, *J. Metamorph. Geol.*, 1993, vol. 11, pp. 241–260.

Pattison, D.R.M. and Newton, R.C., Reversed Experimental Calibration of the Garnet–Clinopyroxene Fe–Mg Exchange Thermometer, *Contrib. Mineral. Petrol.*, 1989, vol. 101, no. 1, pp. 87–103.

Pearce, J.A., Role of the Sub-Continental Lithosphere in Magma Genesis at Active Continental Margins, *Continental Basalts and Mantle Xenoliths*, Hawkesworth, C.J. and Norry, M.J., Eds., Shiva, 1983, pp. 230–272.

Ringwood, A.E., *Composition and Petrology of the Earth's Mantle*, New York: McGraw-Hill, 1975.

Rock, N.M.S. and Leake, B.E., The International Mineralogical Association Amphibole Nomenclature Scheme: Computerization and Its Consequences, *Mineral. Mag.*, 1984, vol. 48, pp. 211–227.

Salters, V.J.M. and Shimizu, N., World-Wide Occurrence of HFSE-depleted Mantle, *Geochim. Cosmochim. Acta*, 1988, vol. 52, pp. 2177–2182.

Saunders, A., Tarney, J., and Weaver, S., Transverse Geochemical Variation across the Atlantic Peninsula: Implications for the Genesis of Calc-Alkaline Magmas, *Earth Planet. Sci. Lett.*, 1980, vol. 46, pp. 344–360.

Schilling, J.G., Zajac, M., Evans, R., *et al.*, Petrologic and Geochemical Variation along the Mid-Atlantic Ridge from 29°N to 73°N, *Am. J. Sci.*, 1983, vol. 283, pp. 510–586.

Schliestedt, M., Eclogite–Blueschist Relationships as Evidenced by Mineral Equilibria in the High-Pressure Metabasic Rocks of Sifnos (Cycladic Islands), Greece, *J. Petrol.*, 1986, vol. 27, no. 6, pp. 1433–1459.

Schulz, B., Mineral Chemistry, Geothermobarometry and Pre-Alpine High-Pressure Metamorphism of Eclogitic Amphibolotes and Mica Schists from the Schobergruppe, Austroalpine Basement, Eastern Alps, *Mineral. Mag.*, 1993, vol. 57, no. 387, pp. 189–202.

Sengupta, P., Dasgupta, S., Bhattacharya, P.K., and Hariya, J., Mixing Behavior in Quaternary Garnet Solid Solution on an Extended Ellis and Green Garnet–Clinopyroxene Geothermometer, *Contrib. Mineral. Petrol.*, 1989, vol. 103, no. 2, pp. 223–227.

Sobolev, A.V., Danyushevskii, L.V., Dmitriev, L.V., *et al.*, High-Aluminum Magnesian Tholeiite: A Primary Melt of Mid-Ocean Ridge Basalts, *Geokhimiya*, 1988, no. 10, pp. 1522–1528.

Sun, S.S. and McDonough, W.F., Chemical and Isotopic Systematics of Oceanic Basalts: Implication for Mantle Composition and Process, *Geol. Soc. London Spec. Publ.*, 1989, pp. 313–345.

Tatsumi, Y., Hamilton, and Nesbitt, R.W. Chemical Characteristics of Fluid Phase Released from a Subducted Lithosphere and the Origin of Arc Magmas: Evidence from High-Pressure Experiments and Natural Rocks, *J. Volcanol. Geotherm. Res.*, 1986, vol. 29, pp. 293–309.

Thoeni, M. and Jagoutz, E., Some New Aspects of Dating Eclogites in Orogenic Belts: Sm–Nd, Rb–Sr, and Pb–Pb Isotopic Results from the Austroalpine Saualpe and Koralpe Type-Locality (Carinthia/Styria, Southeastern Austria), *Geochim. Cosmochim. Acta*, 1992, vol. 56, pp. 347–368.

Velilla, N. and Hach-Ali, P.F., The Composition and Zoning of Metabasite Garnets in the Sierra Nevada (Betic Cordillera, SE Spain), *Neues Jahr. Min. Abh.*, 1986, vol. 154, no. 1, pp. 41–56.

Zakariadze, G.S., Adamiya, Sh.A., Kolcheva, K., *et al.*, Geochemistry of the Metabasic Series of the Pre-Alpine Ophiolites of the Eastern Mediterranean Region, *Petrologiya*, 1993, vol. 1, no. 1, pp. 50–87.